J Fluoresc (2010) 20:203–213
DOI 10.1007/s10895-009-0540-5

ORIGINAL PAPER

Single-Pair Fluorescence Resonance Energy Transfer (spFRET) for the High Sensitivity Analysis of Low-Abundance Proteins Using Aptamers as Molecular Recognition Elements

Wonbae Lee · Anne Obubuafo · Yong-Ill Lee · Lloyd M. Davis · Steven A. Soper

Received: 24 March 2009 / Accepted: 15 September 2009 / Published online: 3 October 2009

Abstract We have developed a strategy for the detection of single protein molecules, which uses single-pair fluorescence resonance energy transfer (spFRET) as the readout modality and provides exquisite analytical sensitivity and reduced assay turn-around-time by eliminating various sample pre-processing steps. The single-protein detection assay uses two independent aptamer recognition events to form an assembly conducive to intramolecular hybridization of oligonucleotide complements that are tethered to the aptamers. This hybridization brings a donor-acceptor pair within the Förster distance to create a fluorescence signature indicative of the presence of the protein-aptamer(s) association complex. As an example of spFRET, we demonstrate the technique for the analysis of serum thrombin. The assay requires co-association of two distinct epitope-binding aptamers, each of which is labeled with a donor or acceptor fluorescent dye (Cy3 or Cy5, respectively) to produce a FRET response. The FRET response between Cy3 and Cy5 was monitored by single-molecule photon-burst detection, which provides high analytical sensitivity when the number of single-molecule events is plotted versus the target concentration. We are able to identify thrombin with high efficiency based on photon burst events transduced in the Cy5 detection channel. We also demonstrate that the technique can discriminate thrombin molecules from its analogue prothrombin. The analytical sensitivity was >200-fold better than an ensemble measurement.

Keywords Single-pair FRET · Aptamers · Thrombin·DNA-protein interactions · Biosensor

W. Lee · A. Obubuafo · S. A. Soper (✉)
Department of Chemistry, Louisiana State University,
Baton Rouge, LA 70803-1804, USA
e-mail: chsope@lsu.edu

Y.-I. Lee
Department of Chemistry, Changwon National University,
Changwon, 641-773, South Korea

L. M. Davis
Center for Laser Applications,
University of Tennessee Space Institute,
Tullahoma, TN 37388, USA

Introduction

With the advent of discoveries emanating from several different proteome projects, new serum-based protein biomarkers are evolving that possess high diagnostic value for a variety of diseases. For example, the early detection and monitoring of prostate-specific proteins, such as prostate-specific antigen (PSA), provides a valuable tool for the management of prostate cancer-related diseases. In practice, men with elevated PSA levels above 10 ng/mL in serum have greater than 50% chance of contracting prostate cancer, while men with 4–10 ng/mL PSA levels are considered as a candidate for prostate biopsy [1, 2].

The common strategy used for the analysis of low-abundance proteins, which cannot be directly amplified like nucleic acids, is typically an immunoassay configured in either a competitive or sandwich-based format with specific monoclonal or polyclonal antibodies labeled with an enzymatic [3], fluorometric [4], or radioactive reporter [5]. While these assay strategies have been very successful, they do have some limitations such as their limited dynamic range, poor analytical sensitivity and the difficulty in detecting extremely low-concentration targets, typically in the range of 100 pM or lower.

Due to the high demand for convenient and sensitive assays appropriate for detecting extremely low-levels of specific proteins in biological samples, new methodologies for the quantification of selected proteins have been developed in the past few years to replace or compliment immunoaffinity-based assays. Examples include molecular beacon assays [6, 7], proximity ligation-based assays [8, 9] and exonuclease protection assays [10, 11].

Proximity ligation assays are particularly attractive because they have the ability to indirectly detect single protein molecules following successful DNA ligation events brought about by recognition elements binding to their respective epitopes on the target protein. The superior limits-of-detection are achieved by amplifying, via PCR, DNA ligation products with the PCR amplicons serving as a protein surrogate reporter [8, 9].

Another sensitive protein detection assay is the exonuclease protection assay developed by Wang and co-workers [11]. In this assay, the protein, such as thrombin, is incubated with two sequence-specific aptamers with exonuclease I added to degrade only the unbound aptamers. The bound aptamers protected from exonuclease I by thrombin indirectly reflect the presence of target protein and can be quantified by real-time PCR with a limit-of-detection (LOD) of ~100 molecules.

Recently, Heyduk et al. developed a molecular beacon approach for the detection of two prokaryotic transcription factors (trpR and lacR) and a human protein (p53), which used a protein concentration-dependent quenching of fluorescence signals as the transduction modality [6]. In this approach, the protein target was incubated with two DNA fragments each containing half of a DNA sequence motif recognizing a binding site on the protein. Annealing of the DNA fragments in the presence of the protein brought donor and quencher molecules into close proximity resulting in fluorescence quenching.

While the aforementioned assays for detecting small quantities of protein biomarkers are elegant, they do possess some limitations that must be addressed, such as the long processing time associated with many and their limited analytical sensitivity. For example, many assays, even those directed toward protein analyses, utilize a PCR amplification step to assist in readout, which can significantly increase processing time due to the limitations associated with conventional block thermal cyclers and the limited degree of quantification due to the characteristics of PCR processes [8, 9, 11]. Therefore, assay strategies that can obviate the need for an amplification step can potentially reduce assay turn-around time and also, increase the dynamic range and sensitivity of the measurement.

A technique that can be employed to assist in reducing assay turn-around time as well as increasing assay sensitivity is single-molecule detection (SMD), which negates the need for amplification steps due to its implicit single-molecule detection capabilities and also versatile configuration schemes such as a continuous flow parallel format system using a microfabricated polymer-based multi-channel fluidic network.[12] For example, Wabuyele and co-workers successfully applied SMD to rapidly discriminate normal DNA from mutated DNA harboring point mutations in genomic DNA in less than 5 min using single-pair FRET (spFRET) [13]. In that report, a ligation step was used to ligate perfectly matched duplexed DNA forming a molecular beacon upon successful ligation, which induced a FRET response due to the close proximity of a donor-acceptor pair in the closed form of the beacon.

Thrombin is a multifunctional serine protease that plays a key role in pro-coagulation and anti-coagulation in the blood clotting cascade. As a pro-coagulant, thrombin activates factors V, VII and XI through a feedback mechanism and converts fibrinogen into insoluble fibrin [14, 15]. It is also known to induce a range of cellular responses including chemotaxis of monocytes and mitogenesis of lymphocytes [16, 17]. Because of its importance in the maintenance of hemostatic balance, its level of generation in the blood can be greatly affected by the onset and progression of certain diseases. The clinically relevant concentration level of thrombin is in the pM to nM range, with only small changes in the concentration associated with its action [18]. As such, analytical methods targeted for thrombin determinations in serum that offer high sensitivity and favorable limits-of-detection are critical in many clinical settings.

Thrombin has two distinct epitopes, a heparin binding exosite and a fibrinogen-binding exosite, which can be selectively used as recognition sites for its molecular analysis [19]. Indeed, many types of recognition elements have been developed for thrombin including aptamer recognition elements that target both exosites [6, 20, 21]. The binding of these aptamers to thrombin has been extensively investigated including their thermodynamic binding constants and specificity [19, 22, 23].

Aptamer-based biomolecular recognition provides a number of unique advantages over more widely used antibody-based probes. For example, aptamers can be selected against certain targets *in vitro* using a process called SELEX (Systematic Evolution of Ligands by EXponential enrichment) for the simple selection and production of large quantities of the necessary aptamer recognition elements [24–26]. Aptamers also provide better chemical stabilities than their antibody counterparts [27, 28].

Recently, Heyduk et al. developed a thrombin detection assay based upon the use of aptamers binding to their respective exosites of this target [28]. The aptamers contained a poly(ethylene glycol) (PEG) linker and complementary DNA sequences (7-mer) that hybridized when the aptamers associated to their respective exosites. Fol-

lowing intramolecular hybridization, a donor-acceptor pair underwent an efficient FRET response that could transduce the presence of thrombin. The authors were able to demonstrate the analytical utility of this assay using ensemble measurements.

The objective of this paper was to design a spFRET assay capable of detecting single protein molecules using thrombin as the model example to provide near real-time readout by forgoing the need of any amplification step prior to readout. The assay strategy (see Fig. 1) was modeled after that reported by Heyduk et al. and employed a pair of aptamers associating to different exosites of thrombin, bringing two DNA complementary sequences into close proximity allowing for their intramolecular hybridization [29]. Following the hybridization event, a FRET response is elicited that could be recorded from a single protein molecule used for quantifying the amount of thrombin present in the sample with high sensitivity and limit of detection (LOD), appropriate for clinical determinations of thrombin due to its low clinical concentration and also, monitor small changes in its concentration associated with its activation [18].

Experimental details

Materials Human α-thrombin and prothrombin were purchased from Haematologic Technologies, Inc. (Essex Junction, VT) and stored at −4 °C in 50% glycerol before use. The aptamer assemblies (see Fig. 1) consisted of the appropriate aptamers targeting the two exosites of thrombin, five 18-atom hexa-ethylene glycol (PEG) spacers and fluorescent dyes serving as either the donor (Cy3) or acceptor (Cy5). 5′-HD1-7mer-Cy3-3′ (5′ GGTTGGTGTGGTTGG-(Spacer18)$_5$-CGCATCT-C6-Cy3-3′), specific for the heparin-binding exosite of thrombin, and 3′-HD22-7mer-Cy5-5′(5′-Cy5-C6-AGATGCG-(Spacer18)$_5$-AGTCCGTGGTA GGGCAGGTTGGGGTGACT-3′), specific for the fibrinogen-binding exosite of thrombin, were

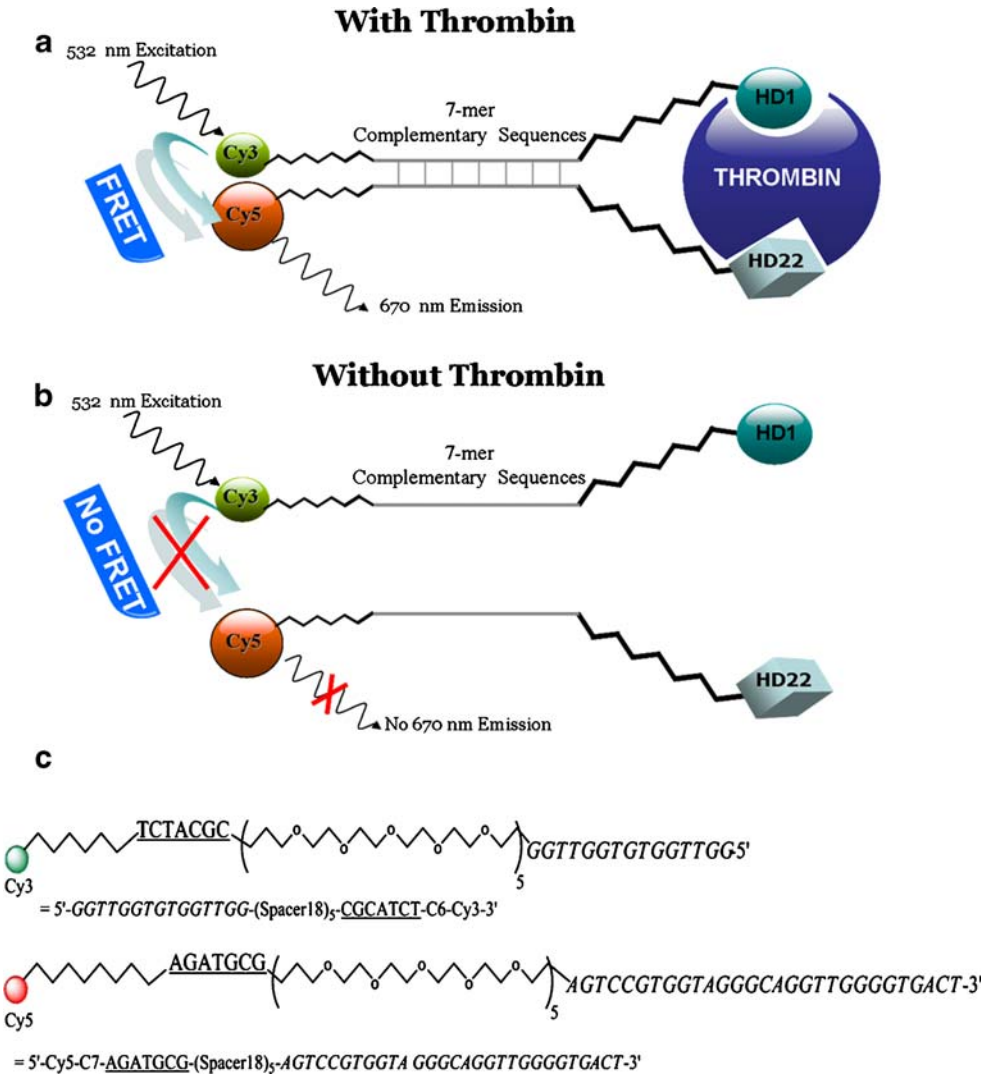

Fig. 1 Schematic view for the molecular recognition of thrombin and its spFRET reporting using the aptamer assemblies. HD1 selectively recognizes the heparin binding exosite of thrombin, while HD22 binds to the fibrinogen binding exosite. (a) In the presence of thrombin, donor (Cy3) and acceptor (Cy5) dyes are brought into close proximity resulting in efficient energy transfer, which is assisted by 7-mer complementary oligonucleotides forming an intramolecular duplex following recognition. (b) Without thrombin, no acceptor fluorescence is produced due to the lack of proximity between the donor-acceptor pair resulting from non-hybridization of the 7-mers. (c) Chemical structures of the two aptamer assemblies containing a PEG linker (C18) and complementary DNA sequences (7-mers, underlined) that hybridized when the aptamers associate to their respective exosites; aptamer sequences are in *italic letters*

custom synthesized by Midland Certified Reagent Company (Midland, Texas) and used as received (see Fig. 1C for structures). The complementary oligonucleotides (7 bases, see underlined sequences in Fig. 1C) were connected to either the 5′ or 3′ end of HD1 or HD22 via five 18-atom hexa-ethylene glycol (PEG) spacers [29]. The complementary oligonucleotides were diluted to the desired concentration and hybridized in Tris saline buffer (TBS) containing 1 mM $MgCl_2$ and 5 mM KCl at pH 8.5. A series of solutions containing the hybridized duplexes were prepared by adding thrombin and in some cases, a prothrombin as well. The reaction mixtures were incubated at room temperature (~20 °C) for 20 mins and a spFRET analysis was initiated by pumping the reaction mixtures through a capillary and subsequently through the excitation laser beam.

Ensemble FRET measurements All bulk fluorescence measurements were carried out using a Fluorolog 3 spectrofluorimeter (HORIBA Jobin Yvon, Inc., Edison, NJ) and absorbance measurements were performed using an Ultrospec 4000 UV/Visible spectrophotometer (Pharmacia Biotech, Cambridge, England) to determine the appropriate excitation/emission wavelengths for the Cy3 and Cy5 labeled oligonucleotides to optimize single-molecule detection of the Cy5 acceptor with minimal interference from the donor. Cy3 and Cy5 end-labeled complementary oligonucleotide sequences were synthesized with or without a PEG internal spacer to evaluate the effects of linker structure on FRET efficiency. The aptamer assemblies were diluted in nuclease-free water from which 1 μM stock solutions in Tris saline buffer (TBS) containing 1 mM $MgCl_2$ and 5 mM KCl at pH 8.5 were prepared. Each oligonucleotide sequence was then combined with its complementary strand in four different combinations depending on the presence or absence of the PEG spacer to a final concentration of 250 nM. The oligonucleotide mixtures were incubated at 37 °C for 1 h and cooled to 4 °C in a RTC-100 thermocycler (MJ Research, Waltham, MA). Fluorescence determinations on the hybridized strands were carried out using a 532 nm excitation wavelength.

Fluorescence measurements were also carried out using a PTI QuantaMaster 4/2006SE spectrofluorimeter (Photon Technology International, Lawrenceville, NJ), which provided thermostatic control of the sample cuvette that was used for determining duplex melting temperatures (T_m). The temperature was controlled by circulating a mixture of ethylene glycol and water at the desired temperature as the heat transfer fluid through the cell holder.

spFRET measurements A 532 nm green solid-state laser (10 mW, GTEC-500-532-10, Lasiris, Inc., Quebec, Canada) was focused through a 40X, 0.75 NA objective (MRH00400, Plan fluor, Nikon) or a 100X, 1.25 NA objective (SPlan100, 1.25, Olympus) into the sample container, which consisted of a 50 μm internal diameter fused silica capillary (TSP050192, Polymicro Technologies, Phoenix, AZ), which was positioned on an XYZ micro-translational stage for positioning the capillary with respect to the laser beam and collection optics. The length of the detection window formed in the capillary by removing the polyimide coating was ~1 cm. The samples were delivered through the capillary using a Harvard apparatus model 22 syringe pump (South Natick, MA).

A dichroic mirror (Z532/780RPC, Chroma Technologies, Rockingham, VT) was used to direct the laser excitation beam into the microscope objective, which subsequently collected the resulting fluorescence with the dichroic mirror transmitting >90% of the fluorescence resulting from Cy5 (560 nm to 700 nm). The fluorescence from Cy5 was further spectrally isolated from the Rayleigh and specularly scattered radiation using longpass (FEL0600, Thorlabs, Newton, NJ) and bandpass filters (XB114, Omega Optical, Brattleboro, VT). The filtered fluorescence was then focused onto the active area (175 μm diameter) of a photon detector using a 20X objective (MRH00200, Plan Fluor, Nikon). A single photon avalanche diode (SPCM-AQR-14, EG&G, Vandreuil, Canada) was used to detect spFRET signals. Dark count rates for the SPCM were <100 cps according to the manufacturer. The avalanche pulses from the SPCM were processed using a counter/timer board (PCI-6602, National Instruments, Austin, TX) having a temporal resolution of 12.5 ns and subsequently analyzed with custom-built software written using LabView 7.0 (National Instruments, Austin, TX).

The counter/timer board was operated in the buffered event counting mode to record the arrival time of each detected photon. An internal 80-MHz clock updated the counter value continuously; each time an electronic pulse from the SPCM arrived at the counter gate, the counter value was stored. This differs from many single-molecule fluorescence acquisition systems that typically record the number of photon events in a user-defined integration period, typically in the range of 100 μs to 10 ms. Recording the arrival time of each photon with a time resolution of 12.5 ns allows one to produce intensity trajectories on any time scale longer than 12.5 ns.

Results and discussion

Design of aptamer assemblies for recognizing thrombin Various combinations of fluorescent donor and acceptor pairs could be incorporated into the dual aptamer assembly set used for

selecting the target protein and directly transducing its presence with the choice predicated on the efficiency of energy transfer, the color of the acceptor emission and a high molar extinction coefficient of the donor at the selected excitation wavelength. Heyduk et al. compared the performances of different combinations of donor-acceptor pairs for ensemble FRET using a dual aptamer configuration, such as fluorescein/dabcyl, fluorescein/Texas Red, Cy3/Cy5, fluorescein/Cy5, and europium chelate/Cy5 [29]. In their report, the maximum FRET signal was obtained from the europium chelate (λ_{abs}=340 nm, λ_{em}=615 nm) [30] and Cy5 (λ_{abs}=650 nm, λ_{em}=670 nm) pair. Note however, that europium Eu^{3+} has a long fluorescence lifetime (>200 ns), which is not beneficial for single-molecule photon-burst detection because it limits the cycle time between the ground and first excited singlet state, which is approximately equal to $1/\tau_f$, where τ_f is the fluorescence lifetime.

The combination of Cy3 and Cy5 were selected as the donor/acceptor pair for the present studies based on several important characteristics, which were critical for maximizing the specificity and signal-to-noise-ratio for the spFRET measurements. For example, the emission range of Cy5 is such that background autofluorescence at its observation wavelength range is often reduced compared to dyes emitting in the blue region of the electromagnetic spectrum [31]. In addition, Cy3 has a high molar extinction coefficient at 532 nm, a common lasing line of a solid-state laser (ε_{exc}=86,000/M·cm) leading to high rates of absorption, k_a, at modest laser powers [32–34]. Finally, the overlap integrals between Cy3 and Cy5 have a rather favorable value (5.5×10^{13} M/cm^3), providing efficient energy transfer between this dye set. Also, to permit direct comparisons of spFRET and ensemble measurements, this dye set was throughout the reported studies.

Effects of linker structures on the FRET response for Cy3 and Cy5 Results of ensemble studies used to optimize the linker architecture for the aptamer assembly to maximize the spFRET response are shown in Fig. 2. These measurements were performed using high concentrations of the aptamer assemblies (1 μM) as well as a relatively low monitoring temperature (~7 °C, Theoretical T_m=~21.5 °C at 1 μM), which assured that the majority of the aptamer assemblies were in their duplexed form (see next section for discussion of thermal melting of duplexed 7-mers). The linker identities included no linker versus an alkane (C6) linker and the presence versus absence of the PEG groups in the linker as well. In these studies, we also considered direct excitation of the acceptor (Cy5 at 532 nm) in the absence of the donor (see Fig. 2) as this can potentially give rise to false positive signals. As can be seen, direct excitation of the Cy5 aptamer assembly at 532 nm excitation resulted in minimal amounts of fluorescence

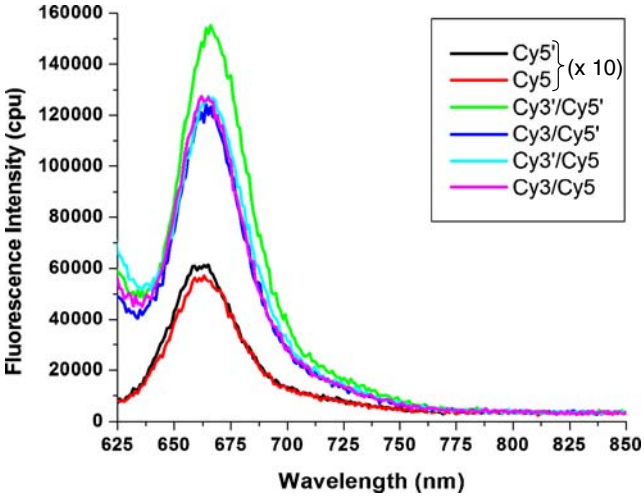

Fig. 2 Ensemble FRET spectra for the aptamer assemblies in which the complementary oligonucleotides were hybridized in TBS buffer at pH 8.5. Excitation was carried out at 532 nm and the fluorescence emission spectra acquired between 625 and 850 nm. Both oligonucleotides were synthesized with the FRET dyes attached with (designated by a prime) or without the PEG internal spacer between the appropriate dye and the oligonucleotide complements. Also shown are the emission spectra of the Cy5 aptamer assembly only using direct excitation at 532 nm. These spectra have been multiplied by 10-fold to improve clarity. The aptamer assembly concentrations used here was 1 μM with all measurements made at ~7 °C

irrespective of the presence or absence of the PEG linker, which is consistent with the low molar absorptivity of Cy5 at this excitation wavelength.

When the complementary sequences (7-mers) were predominately in the duplexed form with the linkers containing or not containing the C6 structure used to attach the fluorescent dyes to the aptamer assemblies, relatively equal FRET responses resulted (see Fig. 2). However, when both aptamer assemblies contained the PEG linkers and the C6 linkers, slightly larger amounts of FRET signals were generated. Therefore, our spFRET measurements were carried out using the C6 linkers containing the PEG groups.

Theoretical and experimental melting temperature (T_m) of 7-mer complementary oligonucleotides We conducted experiments to determine the T_m of the 7-mer complementary oligonucleotide sequences attached to the aptamer assemblies used to bring the donor-acceptor pair into close proximity following aptamer(s) recognition of the target in order to undergo FRET. To optimize the spFRET response and minimize false positive or negative results, the 7-mer complementary oligonucleotides should have two main features: (1) the oligonucleotides have a significantly different T_m following aptamer binding to their respective exosites of the target compared to the oligonucleotides when the aptamers are in their non-associated state; (2) following hybridization of the 7-mers, the donor (Cy3) and acceptor (Cy5) dyes are brought into close proximity to

maximize the FRET response. Also, if hybridization of the complementary oligonucleotides occurs in the absence of thrombin, the experimental results can lead to false positives. Therefore, it was essential to compare experimental and theoretical T_m values for the 7-mer complementary sequences.

There are several algorithms that can be effectively used for calculating T_m, most of which take into account solution and oligonucleotide conditions to determine the thermodynamic properties of the hybrids. Briefly, the T_m is a function of the GC/AT ratio, fragment length, nucleotide sequence, concentration of the oligonucleotides and the ionic strength and ion identity in terms of the solution conditions. In this study, the T_m of the 7-mer oligonucleotides were analyzed using the DINAMelt Software (http://www.bioinfo.rpi.edu/applications/hybrid/hybrid2.php) [35]. To verify the theoretical T_m values, we collected ensemble donor and acceptor fluorescence from a sample containing equimolar amounts of the two aptamer assemblies with or without thrombin under the same buffer conditions as those used for the spFRET measurements.

We first carried out ensemble FRET measurements of the aptamer assemblies in the absence and presence of thrombin (5 nM) by plotting the ratio of acceptor/donor fluorescence intensity as a function of temperature with the results of these investigations displayed in Fig. 3. In both cases, the curves yielded a sigmoidally-shaped profile with the acceptor/donor ratio increasing at lower temperatures when the aptamer assemblies were either in the absence or presence of thrombin. The results indicated that the complementary 7-mers displayed increased thermodynamic stability in the presence of thrombin compared to the case when no thrombin was present due to differences in their T_m's (T_m~9 °C with no thrombin; T_m ~19 °C with thrombin). This can be explained by the fact that intramolecular duplexes have higher thermodynamic stability compared to intermolecular duplexes, especially at relatively low oligonucleotide concentrations as those used here [36]. In the presence of thrombin, the aptamers associate to their respective exosites and thus form a molecular assembly to allow for the intramolecular hybridization of the 7-mer complements whereas in the absence of thrombin, the hybridization remains as an intermolecular process. For our spFRET measurements, the selected measurement temperature was 20 °C, slightly above the T_m for the aptamer assemblies in the presence of thrombin (see Fig. 3). While this will reduce false positive results by minimizing the number of hybrids formed for the 7-mers in the absence of thrombin, it can effectively melt nearly 50% of the hybrids formed in the presence of thrombin, increasing the false negative rate, because this temperature is close to the T_m of the association complex.

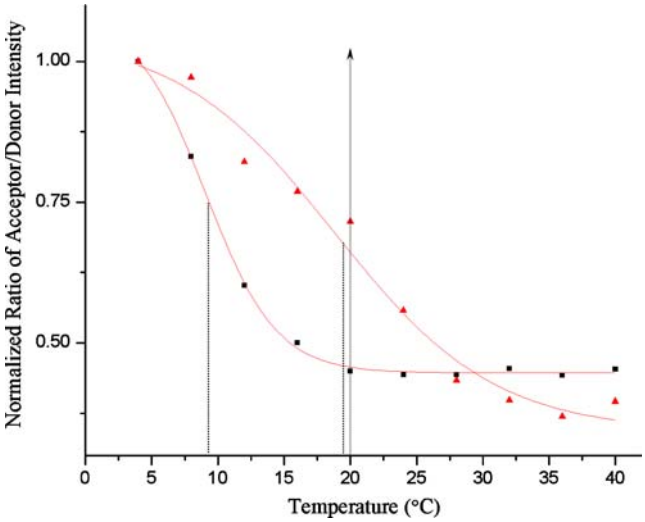

Fig. 3 Normalized fluorescence melting curves for the 7-mer complementary oligonucleotides of the aptamer assemblies as a function of temperature, which was determined by ensemble FRET measurements generated from the donor-acceptor pair. The fluorescence was corrected for the temperature dependent emission exhibited by both dyes. The data shows the melting profiles for the aptamer assemblies in the presence (triangles) and absence (squares) of thrombin. The spectra were acquired using equimolar amounts of the aptamer assemblies and thrombin (5 nM). The emission was collected on a fluorescence spectrometer equipped with a thermostated cuvette using an excitation wavelength of 532 nm. The solid line represents the best fit function to the data (sigmoidal function). The solid arrow line designates the temperature at which the spFRET measurements were made while the dotted lines represent the T_m's for the 7-mer oligonucleotides in the absence and presence of thrombin

Because the T_m is a thermodynamic quantity, its value is concentration dependent, at least for intermolecular hybrids. Based on theoretical calculations using DINAMelt, the T_m of the 7-mer complementary sequences was determined to be 4.9 °C at 5 nM compared to the value of approximately 21 °C at 250 nM. The parameters used for the T_m calculations with the DINAMelt were: energy rules for DNA, $[Na^+]$=100 mM, $[Mg^{2+}]$=1 mM, and a non-polymer mode. However, as noted above, the T_m value becomes independent of concentration when the complementary sequences hybridize intramolecularly. Therefore, it is particularly advantageous to perform the FRET measurements with low aptamer assembly concentrations to provide a large difference in the T_m of the unassociated and associated aptamer assemblies to minimize the number of false positive signals.

It should be noted that the experimental T_m for the aptamer assemblies in the absence of thrombin was found to be ~9 °C (see Fig. 3), but the calculated value was found to be 4.9 °C. We are uncertain at this time of why these values differ, but plausible explanations could be the effects of the linker structures on the hybrid stability (not included in the DINAMelt calculations) or the effects of additional salts used in the experiments compared to the theoretical calculations.

Working concentrations of aptamer assemblies for spFRET The excitation laser beam creates a small open volume element called the probe or detection volume [37]. When a fluorescent molecule passes through the probe volume, the molecule will be cycled between its ground and electronic states with electronic relaxation producing fluorescence. The number of these excitation/emission cycles is determined by the irradiance, transit time and the dye's photostability, fluorescence lifetime and absorption cross section. Generally, single-molecule experiments require the probability of single-molecule occupancy within the detection volume to be smaller than unity to statistically lower the probability of double occupancy [13]. This can be achieved using fluorescent reporters of low concentration and/or small probe volumes. The probability of occupancy (P_0) can be calculated from

$$P_0 = CN_A P_V \tag{1}$$

where C is the analyte concentration, P_V is the size of the probe volume, and N_A is Avogadro's number. To assure that the observed signals are indeed due to single molecules, the temporal average of the particle number inside the probe volume should be <0.1 [38].

In our spFRET thrombin assay, the target single-molecule concentration is the association complex concentration, which is determined by the binding affinity (K_a, association constant), aptamer concentration, and thrombin concentration according to the following expression:

$$HD1 + HD22 + Thrombin \underset{Kd}{\overset{Ka}{\rightleftharpoons}} HD1 \cdot Thrombin \cdot HD22 (triplex)$$

Based on published literature values, the K_d between HD1 (15-mer) and thrombin is 25–450 nM, whereas the K_d between HD22 (29-mer) and thrombin is ~0.5 nM [21,39]. The single-molecule occupancy in the present case is determined primarily by the associated triplex concentration, which in turn is determined by the aptamer and thrombin concentrations as well as the equilibrium constant for association/dissociation (K_a or K_d).

To determine an acceptable aptamer concentration to make sure we operate in a regime of high single-molecule occupancy probability and yet satisfy the thermodynamic constraints imposed by the equilibrium expression above, we measured the probe volume to allow the evaluation of an acceptable concentration of material using Eq. (1). The probe volume size was determined from the average transit time, τ_t, of fluorescent beads moving through the probe volume. The transit time was estimated from an autocorrelation analysis of a single bead data stream [40]. The $1/e^2$ beam radius (ω_0) was determined from the transit time (4.8 ms) with the volumetric flow rate used in the experiment (linear velocity, v, was 0.08 cm/s based on the cross sectional area of the capillary tube and the input volumetric flow rate) using the equation, $\tau_t=(\pi\omega_0)/2v$, and yielded a value of 2.4 μm for the beam waist (ω_o) [41]. The effective probe volume, V, could be calculated using, $V=\pi^{3/2}\omega_0^2 z_0$, where z_o is the confocal length (half-depth of focus of the relay objective) [42]. An upper limit for the effective probe volume would be ~0.8 pL if it is assumed that z_o=25 μm (radius of capillary tube, because a pinhole was not used in the secondary image plane of the relay objective). Using Eq. (1), we could therefore use an aptamer assembly concentration of ~0.1 pM to remain in the single-molecule occupancy regime assuming that the aptamers are the limiting reagents and the K_a is large enough to favor the formation of the complex.

However, the experimental results for the use of 0.1 pM concentrations of the aptamer assemblies showed no evidence of photon burst events on the Cy5 acceptor channel irrespective of the thrombin concentration employed. While we are not certain of the K_a value for the equilibrium expression shown above, the use of these small concentration values for the aptamers did not seem to favor formation of the association complex to any appreciable amount.

In order to increase the working concentrations of the aptamer assemblies to drive the equilibrium toward the association complex, which is the actual species that is being transduced, the probe volume was further reduced by introducing a pinhole in the secondary image plane of the optical path using a 100X, 1.25 NA objective (SPlan100, 1.25, Olympus). This new probe volume was found to have a volume of ~0.055 fL if only considering the central cylindrical volume, and ~0.69 fL if a more applicable Gaussian model was imposed [43]. Using this probe volume size, we were required to increase the working concentration of the aptamer assemblies up to ~5.0 nM to observe spFRET photon bursts arising from the association complex (see Eq. (1)). Assuming all of the aptamers and thrombin exist as the triplex, the mean occupancy number of the triplex molecules resident in the optical probe volume of 0.69 fL would be 2.07, which would show no evidence of single photon burst events and an increase in the average background level [43]. As can be seen in Fig. 4, the average background level did not increase at this aptamer assembly concentration and discrete burst events were clearly evident, indicating that the mean occupancy is significantly less than the number calculated based on the aptamer assembly concentration.

Specificity of thrombin spFRET detection A series of "blank" solutions were analyzed using single-molecule photon-burst detection to address the question of whether the 7-mer complementary sequences appended to each recognition aptamer would hybridize in the absence of thrombin. The presence of photon burst signatures would arise from either energy transfer between the donor-

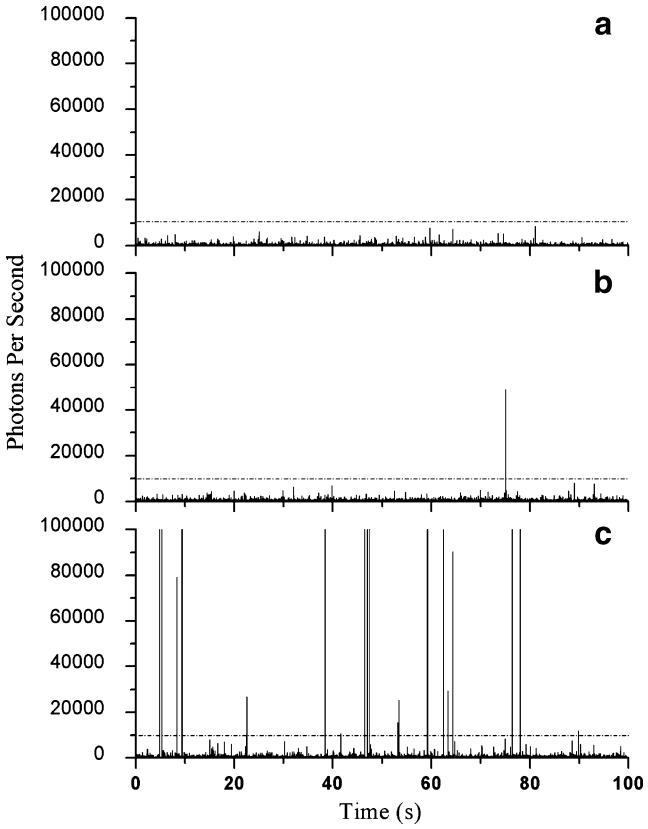

Fig. 4 Raw data of spFRET events for the single molecule detection of thrombin. The average number of events were registered as those above the threshold level (10,000 s^{-1}), which is shown as the dotted line in each panel. Aptamer assembly solutions (5 nM 5′-HD1-7mer-Cy3-3′+ 5 nM 3′-HD22-7mer-Cy5-5′) were incubated with thrombin for approximately 20 mins before loading into the flow cell and monitoring the single-molecule burst data (buffer conditions: 50 mM Tris at pH 8.5, 100 mM NaCl, 5 mM KCl, and 1 mM $MgCl_2$). (a) Buffer only; (b) 5 nM 5′-HD1-7mer-Cy3-3′ + 5 nM 3′-HD22-7mer-Cy5-5′; (c) 5 nM 5′-HD1-7mer-Cy3-3′ + 5 nM 3′-HD22-7mer-Cy5-5′ + 5 nM thrombin. The experiments were carried out using 532 nm excitation (30 μW). The solutions were hydrodynamically driven through the probe volume using a syringe pump at a linear flow rate of 0.08 cm/s

acceptor pair following self-hybridization of the 7-mer complementary sequences contained in the aptamer assemblies or direct excitation and emission of the donor or acceptor. To perform these measurements, a preset threshold value was selected, which was determined by evaluating data from buffer solutions only (see Fig. 4A) and was selected high enough to produce no false positive signals from this buffer. The optimum value for this threshold maximizes detection efficiency and, at the same time, minimizes false positive signals [41]. In the data acquisition software, the photoelectron events were processed by subjection to a weighted sliding sum filter for improving the ability to distinguish between photon bursts generated from single molecules and those from random fluctuations in the background [44]. The time-width of the filter selected here corresponded to the average molecular transit time with the weighting factors selected to model a Gaussian function due to the Gaussian laser beam profile.

As can be seen in Fig. 4B, only a single photon-burst-event appeared above the discriminator threshold (10,000 counts/s) for the Cy5 (acceptor) detection channel when the buffer containing the aptamer assemblies and no thrombin was analyzed (collection time T=100 s). From previous theoretical and experimental results, the melting temperature of the 7-mer complementary sequences at 5.0 nM was estimated to be ~4.9 °C. Therefore, at room temperature the complementary sequences in the absence of thrombin should be predominately in their single-stranded form and thus, based on proximity considerations, only a very small number of occurrences of FRET would be expected.

To evaluate the ability of the aptamer assemblies to transduce the presence of thrombin using spFRET, we spiked thrombin into a solution containing a final concentration of 5 nM of each of the two aptamer assemblies at a concentration of 5 nM as well. As can be seen from Fig. 4C, a number of photon-burst events were found to exceed the preset molecular discriminator threshold and possessed a diverse range of amplitudes due to the fact that the association complexes could move through the Gaussian beam on the wings, where the fluence is reduced and as such, the excitation rate and photon yield drops. Over the 100 s time period displayed in the panel shown in Fig. 4C, 20 events were detected. Unfortunately, we cannot calculate the number of expected events based on the concentration of the molecular species, the probe volume size and the linear velocity as is done in most flow-based single molecule experiments due to the fact that the thrombin:aptamers association complex concentration is thermodynamically controlled and we are uncertain of the valve of K_a. It should be noted as well that the single-molecule measurement temperature (see solid arrow in Fig. 3) is close to the T_m of the complementary sequences contained in the aptamer assemblies in the presence of thrombin and as such, approximately 50% of the expected response may be lost due to duplex melting. In addition, at the thrombin concentration employed here (*i.e.*, comparable to the aptamer assembly concentrations), we may have thrombin molecules that have only one of their exosites filled, giving rise to false negative signals because these complexes would not produce a spFRET response. Using thrombin concentrations below the aptamer assembly concentrations would alleviate this source of error.

We further explored the specificity of spFRET analysis by testing solutions containing prothrombin under the same experimental conditions as that used for thrombin and compared these results to the thrombin solutions. The histograms in Fig. 5 show the average number of spFRET

events (five replicates) above threshold that were observed for each of the samples tested. As can be seen from the results depicted in Fig. 5, single-molecule events were observed for prothrombin, but at a much lower frequency compared to thrombin. This result is consistent with previous experimental results obtained by Heyduk et al., in which prothrombin could be recognized by these aptamer sensors but with much reduced (>20-fold) limit-of-detection compared to thrombin, which results from its expected lower K_a compared to thrombin [29].

Sensitivity of the spFRET measurements Calibration plots were next constructed using spFRET and ensemble FRET measurements for thrombin using the aptamer assemblies depicted in Fig. 1. For the spFRET measurements, the number of photon-burst events versus the thrombin concentration was used while for the ensemble measurements, the fluorescence intensity versus thrombin concentration was plotted. The resulting calibration plots are shown in Fig. 6, with error bars obtained from four replicates. Analysis of the calibration plots indicated a thrombin concentration limit-of-detection of 48 nM for the ensemble measurement (three standard deviation units above background). In the case of the spFRET measurements, the assay could detect a single thrombin molecule based on the fluorescence signal-to-noise ratio. However, the concentration detection limit for thrombin is set by thermodynamic considerations with a larger K_a providing a better concentration limit-of-detection.

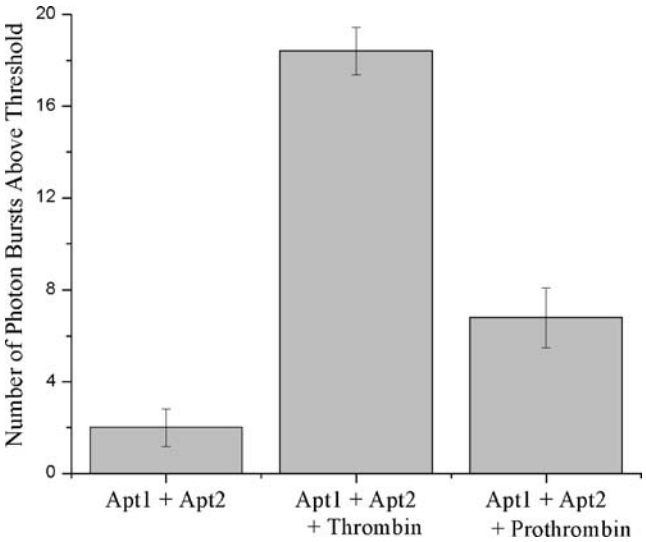

Fig. 5 Comparison of the average number (five replicates for each 100 s assay) of single-molecule events on various combinations of samples showing the selectivity of the aptamers assemblies for thrombin. The final concentrations of the samples were 5 nM with the same concentrations used for both aptamer assemblies, thrombin, and prothrombin

The analytical sensitivity of these measurements was determined for the ensemble FRET and the spFRET measurements. We found that a 57% relative change per nM in analytical signal resulted for the spFRET measurements while the ensemble FRET measurements only produced a sensitivity value of 0.2% per nM. The relative change in the analytical signal was calculated as

$$\Delta\text{signal}/\ \langle\text{signal}\rangle \tag{2}$$

and was normalized to the concentration of thrombin (nM); Δsignal = the change in signal between two data points in the calibration plot and <signal> is the average signal of the same two data points. As can be seen from this data, the analytical sensitivity normalized to the concentration is

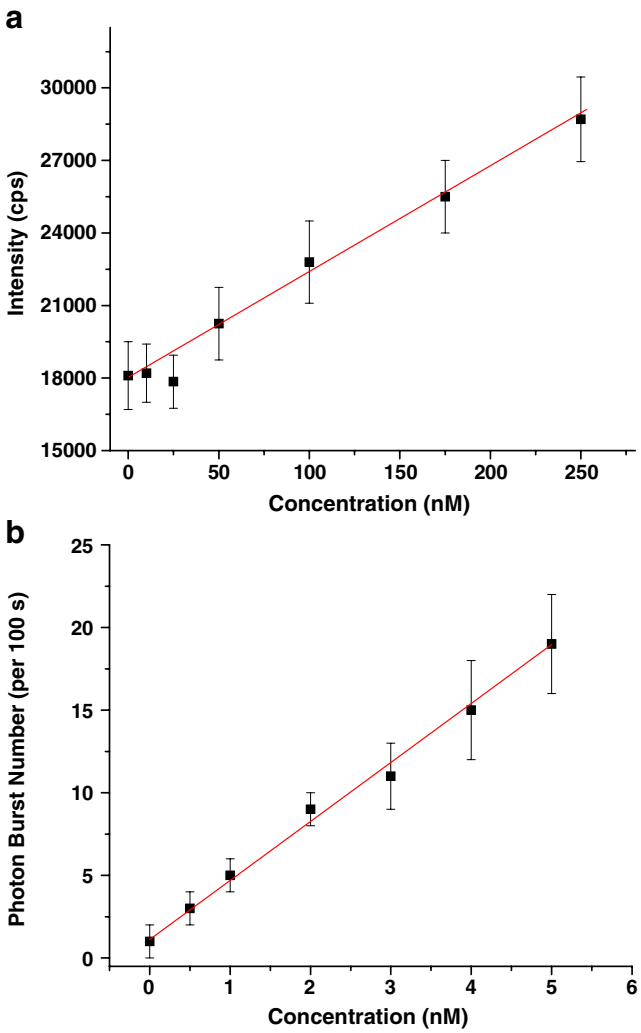

Fig. 6 (a) Calibration curve showing the ensemble FRET response as a function of various concentrations of thrombin run in a TBS buffer at pH 8.5. The 5′-HD1-7mer-Cy3-3′ and 3′-HD22-7mer-Cy5-5′ concentrations were fixed at 250 nM. (b) Calibration plot showing the average number of spFRET events versus the concentration of thrombin. The aptamer assembly concentrations used throughout these measurements was 5 nM

much greater for the spFRET measurements compared to the ensemble measurements. Therefore, much smaller changes in thrombin concentration can be accurately discerned using the single-molecule readout strategy compared to ensemble measurements.

Conclusions

In this study, we evaluated the performance of a spFRET system for the detection of single protein molecules using thrombin as a model and demonstrated the advantages of direct single-molecule readout without the need of any amplification step prior to readout. The assay was successfully coupled to a dual aptamer molecular recognition event to provide high specificity for the detection phases of the assay [28]. This dual molecular recognition process allowed for distinguishing thrombin from its zymogen analogue, prothrombin. In addition, the ability to transduce the presence of single protein molecules using photon-burst detection provided high analytical sensitivity. While other strategies have been reported for the single-molecule analysis of protein molecules, for example the proximity ligation-based assay, most require an intervening PCR amplification step with indirect readout accomplished via PCR amplicons following a successful ligation event. The assay reported herein eliminates the need for the PCR amplification step and can provide near real-time readout with the only sample pre-processing requirement being an incubation step for allowing the molecular associations to occur followed by on-line spFRET detection. While the current spFRET measurements used a 20-minute incubation step, this incubation time can be significantly reduced using small reaction volumes (*i.e.*, lower diffusional distances) and/or active mixing, such as those typically employed in many microfluidic platforms.

In the present example, a single target molecule was analyzed using this assay format, which employed a flow-through system with photon burst detection of spFRET events. However, in many clinical applications, multiple markers must be simultaneously analyzed using a multiplexed format. We have recently reported a system that can perform spatial multiplexing using a flow-based single-molecule detection approach [45]. Therefore, the single-molecule assay reported herein can be configured using microfluidics and an imaging CCD to perform multiplexed clinical measurements in which a panel of markers from a single sample can be simultaneously analyzed in near real-time.

Finally, while the fluorescence limit-of-detection was reported to be at the single-molecule level (see data in Fig. 4), the actual concentration detection limit of the target, which in this case is thrombin, depends intimately on the thermodynamic properties of the association complex with tighter binding molecular recognition elements improving this limit-of-detection. Therefore, the use of higher affinity recognition elements for the selected targets will be particularly attractive for improving the concentration limit-of-detection. It should be noted that while aptamers were used here, any recognition element can be used such as antibodies or peptoids. The only requirement is that the target contains at least two different unique binding sites.

Acknowledgment The authors acknowledge financial support of this work through the National Institutes of Health (EB-006639), the National Science Foundation (EPS-0346411) and the Louisiana Board of Regents.

References

1. Mikolajczyk SD, Rittenhouse HG (2002) Presented at the 1274th Meeting of the Keio Medical Society in Tokyo
2. Tchetgen MB, Oesterling JE (1997) Urol Clin North Am 24:283
3. Christensson A, Laurell CB, Lilja H (1990) Eur J Biochem 194:755
4. Diamandis EP, Yu H (1997) Urol Clin North Am 24:275
5. Critz FA, Williams WH, Benton JB, Levinson AK, Holladay CT, Holladay DA (2000) J Urol 163:1085
6. Heyduk T, Heyduk E (2002) Nature Biotechnol 20:171
7. Tan W, Wang K, Drake TJ (2004) Curr Opin Chem Biol 8:547
8. Fredriksson S, Gullberg M, Jarvius J, Olsson C, Pietras K, Gústafsdóttir SM, Östman A, Landegren U (2002) Nature Biotechnol 20:473
9. Gullberg M, Fredriksson S, Taussig M, Jarvius J, Gústafsdóttir S, Landegren U (2003) Curr Opin Biotechnol 14:82
10. Wang J, Li T, Guo X, Lu Z (2005) Nucleic Acids Res 33:e23
11. Wang XL, Li F, Su YH, Sun X, Li XB, Schluesener HJ, Tang F, Xu SQ (2004) Anal Chem 76:5605
12. Okagbare P, Soper S (2009) The Analyst 134:97
13. Wabuyele MB, Farquar H, Stryjewski W, Hammer RP, Soper SA, Cheng YW, Barany F (2003) J Am Chem Soc 125:6937
14. Davie EW, Fujikawa K, Kisiel W (1991) Biochemistry 30:10363
15. Gosalia DN, Denney WS, Salisbury CM, Ellman JA, Diamond SL (2006) Biotechnol Bioeng 94:1099
16. Bizios R, Malik B (1986) J Cell Physiol 128:485
17. Bar-Shavit R, Hruska KA, Kahn AJ, Wilner GD (1986) Ann NY Acad Sci 485:335
18. Brummel-Ziedins KE, Vossen CY, Butenas S, Mann KG, Rosendaal FR (2005) J Thromb Haemost 3:2497
19. Tasset DM, Kubik MF, Steiner W (1997) J Biol Chem 272:688
20. Bichler J, Heit JA, Owen WG (1996) Thromb Res 84:289
21. Kim Y, Cao Z, Tan W (2008) Proc Natl Acad Sci USA 105:5664
22. Kretz CA, Stafford AR, Fredenburgh JC, Weitz JI (2006) J Biol Chem 281:37477
23. Stubbs MT, Bode W (1995) Trends Biochem Sci 20:23
24. Ellington AD, Szostak JW (1990) Nature 346:818
25. Tuerk C, Gold L (1990) Science 249:505
26. Gold L, Polisky B, Uhlenbeck O, Yarus M (1995) Annu Rev Biochem 64:763
27. Tombelli S, Minunni M, Mascini M (2005) Biosens Bioelectron 20:2424
28. Nimjee SM, Rusconi CP, Sullenger BA (2005) Annu Rev Med 56:555
29. Heyduk E, Heyduk T (2005) Anal Chem 77:1147
30. Marriott G, Heidecker M, Diamandis EP, Yan-Marriott Y (1994) Biophys J 67:957

31. Mosiman VL, Patterson BK, Canterero L, Goolsby CL (1997) Cytometry (Comm Clin Cytometry) 30:151
32. Park JW (2005) Cytometry Part A 65:148
33. Berlier JE, Rothe A, Buller G, Bradford J, Gray DR, Filanoski BJ, Telford WG, Yue S, Liu J, Cheung CY (2003) J Histochem Cytochem 51:1699
34. Mathies RA, Peck K, Stryer L (1990) Anal Chem 62:1786
35. Markham NR, Zuker M (2005) Nucleic Acids Res 33:577
36. SantaLucia J Jr (1998) Proc Natl Acad Sci USA 95:1460
37. Maiti S, Haupts U, Webb WW (1997) Proc Natl Acad Sci USA 94:11753
38. Schwille P, Haustein E (2001) Biophysics Textbook Online: 1
39. Bock LC, Griffin LC, Latham JA, Vermaas EH, Toole JJ (1992) Nature 355:564
40. Soper SA, Shera EB, Martin JC, Jett JH, Hahn JH, Nutter HL, Keller RA (1991) Anal Chem 63:432
41. Soper SA, Mattingly QL, Vegunta P (1993) Anal Chem 65:740
42. Boukari H, Nossal R, Sackett DL (2003) Biochemistry 42:1292
43. Hill E, de Mello A (2000) The Analyst 125:1033
44. Bunfield DH, Davis LM (1998) Appl Opt 37:2315
45. Emory JM, Soper SA (2008) Anal Chem 80:3897